Phase Separation Kinetics and Cluster Dynamics in Active Brownian Systems

Leticia F. Cugliandolo

Sorbonne Université

leticia@lpthe.jussieu.fr

www.lpthe.jussieu.fr/˜leticia

Work in collaboration with

C. Caporusso, **G. Gonnella**, **P. Digregorio**, **G. Negro**, **I. Petrelli**, **M. Semeraro** (Bari), **A. Tiribocchi** (Roma), **L. Carenza** (Bari & Istanbul), **A. Suma** (Trieste, Philadelphia & Bari), **D. Levis & I. Pagonabarraga** (Barcelona & Lausanne)

MIT, USA, 2024

Active Matter

Definition

Active matter is composed of large numbers of active "agents", which consume energy and thus move or exert mechanical forces

Due to the energy consumption, these systems are intrinsically out of thermal equilibrium

Homogeneous energy injection (not from the borders, *cfr.* shear)

Coupling to the environment (bath) allows for dissipation

Active Matter

Natural & artificial systems

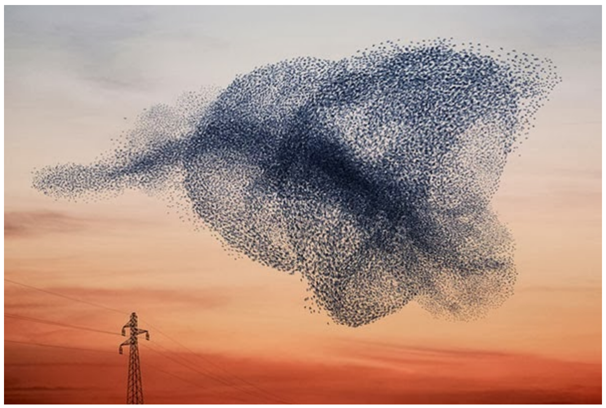

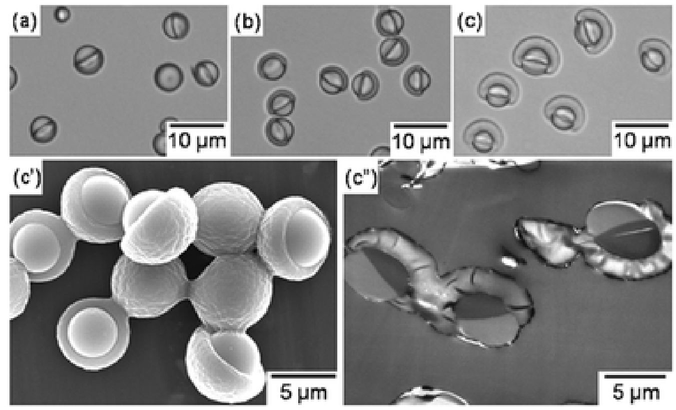

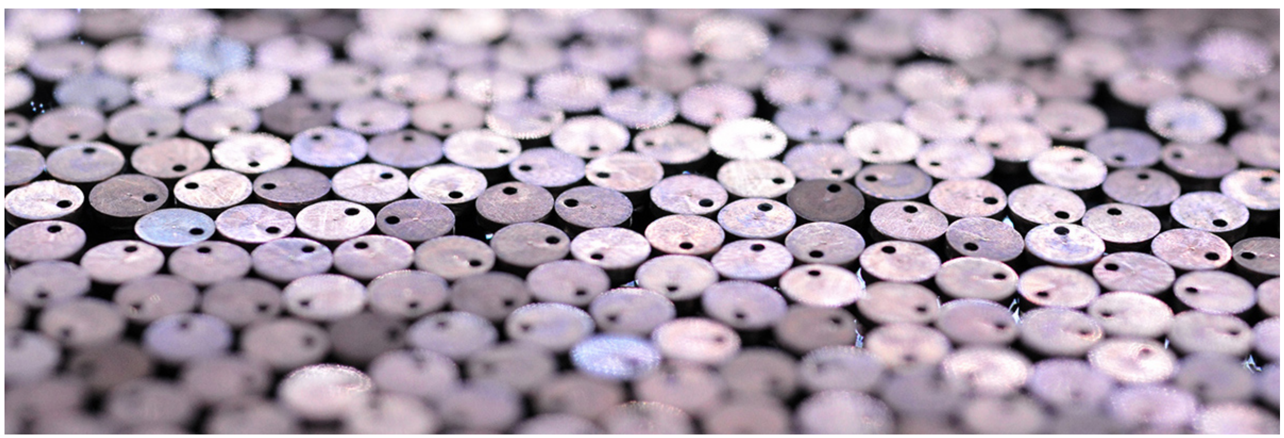

Experiments & observations **Bartolo et al.** Lyon, **Bocquet et al.** Paris, **Cavagna et al.** Roma, **di Leonardo et al.** Roma, **Dauchot et al.** Paris, just to mention some Europeans

Active Matter

Global goal

To understand the collective behaviour **active matter**

from the **statistical physics** viewpoint

with the help of extensive **numerical simulations**

and **analytic arguments**

Statistical Physics approach

2d Active Matter

Why two dimensions ?

It is **experimentally** ‘easier’ than three dimensions

It is computationally lighter to **simulate** $2d$ systems than $3d$ ones

It is already very rich

Two kinds of active constituents

Disks

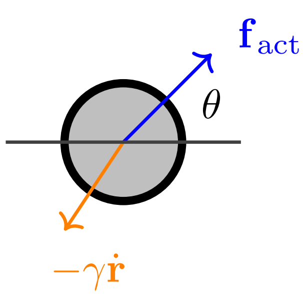

Rigid Dumbbells

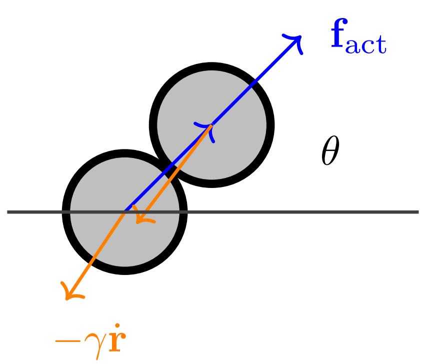

Active Brownian Matter

Questions – à la Statistical Physics – on bidimensional systems

- Activity (Pe) - packing fraction (ϕ) phase diagram.

- Order of, and mechanisms for, the phase transitions.

  — Correlations, fluctuations.

  — Topological defects.

- (Motility Induced) Phase Separation.

  — Internal structure of dense phase.

  — Mechanisms for growth of dense phase.

- Influence of particle shape, *e.g.* disks *vs.* dumbbells.

Active Brownian Matter

Table with results

	Disks	Dumbbells
Non-eq Steady-State		
Approach to NESS		

Active Brownian Matter

Table with results

	Disks	Dumbbells
Non-eq Steady-State	**Next**	
Approach to NESS		

Active Brownian Disks

(Overdamped) Langevin equations

Active force $f_{\rm act}$ along $\mathbf{n}_i = (\cos\theta_i, \sin\theta_i)$

$$m\ddot{\mathbf{r}}_i + \gamma\dot{\mathbf{r}}_i = f_{\rm act}\mathbf{n}_i - \nabla_i \sum_{j(\neq i)} U_{\rm Mie}(r_{ij}) + \boldsymbol{\xi}_i \ , \qquad \dot{\theta}_i = \eta_i \ ,$$

$\mathbf{r}_i$ position of the ith particle & $r_{ij} = |\mathbf{r}_i - \mathbf{r}_j|$ inter-part distance,

$U_{\rm Mie}$ **short-range strongly repulsive** Mie potential

Over-damped dynamics $m/\gamma = 0.1$

$\boldsymbol{\xi}_i$ and η_i Gaussian white noises with $\langle \xi_i^a(t)\rangle = \langle \eta_i(t)\rangle = 0$,

$\langle \xi_i^a(t)\,\xi_j^b(t')\rangle = 2\gamma k_BT\delta_{ij}^{ab}\delta(t-t')$ with $k_BT = 0.05$, and $\langle \eta_i(t)\,\eta_j(t')\rangle = 2D_\theta\delta_{ij}\delta(t-t')$

Persistence time $\tau_p = D_\theta^{-1} = \gamma\sigma^2/(3k_BT)$. Units of length σ and energy ε.

Péclet number $\boxed{\text{Pe} = f_{\rm act}\sigma/(k_BT)}$ measures the activity and

$\boxed{\phi = \pi\sigma^2 N/(4S)}$ the packing friction

Active Brownian Disks

The typical motion of particles in interaction

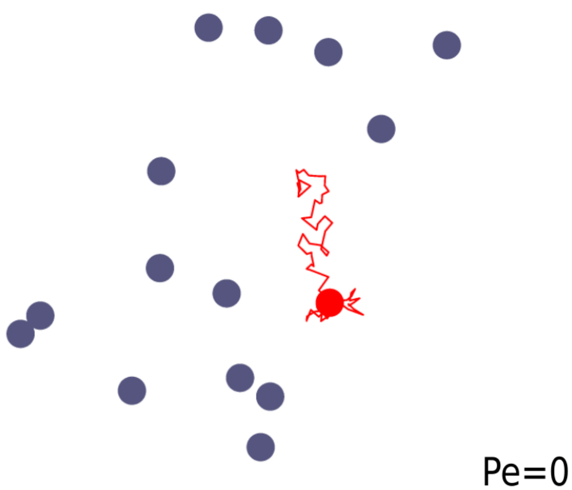

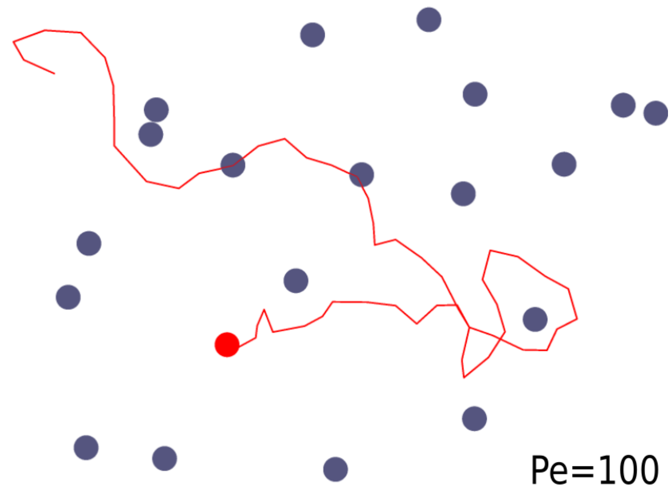

The active force induces a persistent random motion due to

$$\langle \mathbf{f}_{\rm act}(t) \cdot \mathbf{f}_{\rm act}(t') \rangle \propto f_{\rm act}^2 \, e^{-(t-t')/\tau_p}$$

with $\tau_p = D_\theta^{-1} = {}^{\gamma\sigma^2}\!/_{3k_BT}$

Phase Diagram - ABP

Solid, hexatic, liquid, co-existence and MIPS

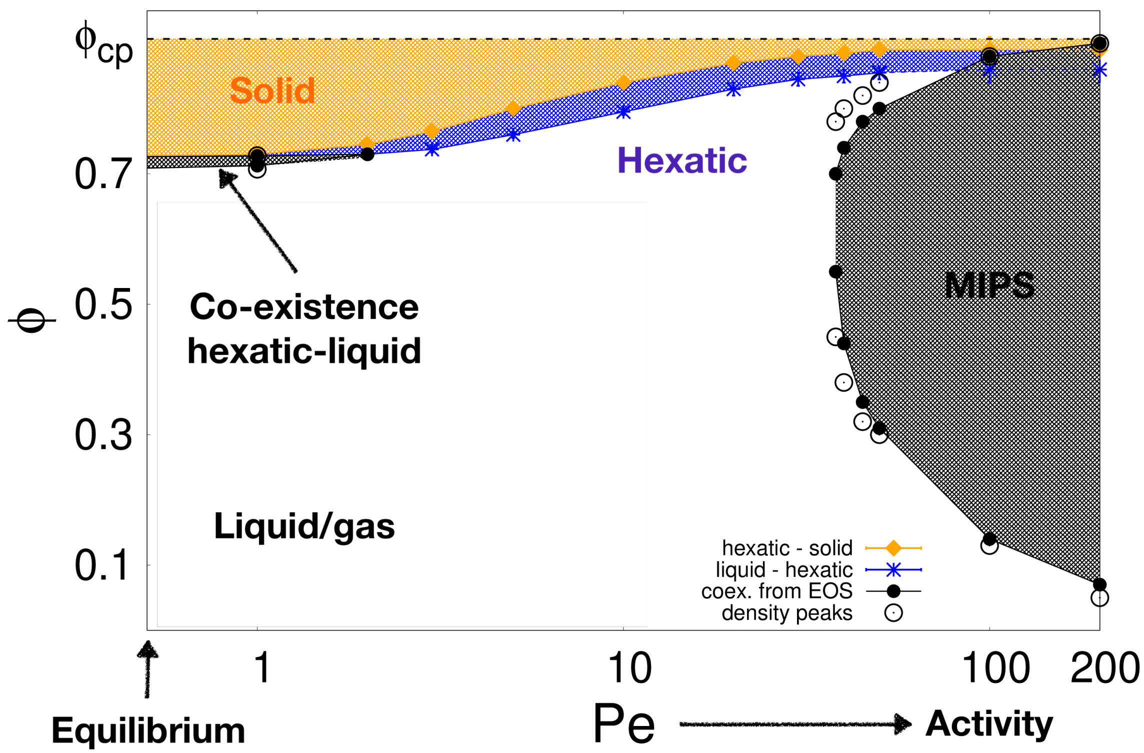

Motility induced

phase separation (MIPS)

gas & dense

Cates & Tailleur

Ann. Rev. CM 6, 219 (2015)

Farage, Krinninger & Brader

PRE 91, 042310 (2015)

Pressure $P(\phi, \mathrm{Pe})$ (EOS), correlations $G_T(r)$, $G_6(r)$, and distributions of ϕ_i, $|\psi_{6i}|$

Digregorio, Levis, Suma, LFC, Gonnella & Pagonabarraga, PRL 121, 098003 (2018)

MIPS - ABP

The basic mechanism

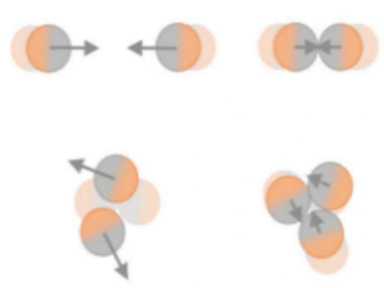

Particles collide heads-on

and cluster even in the

absence of attractive forces

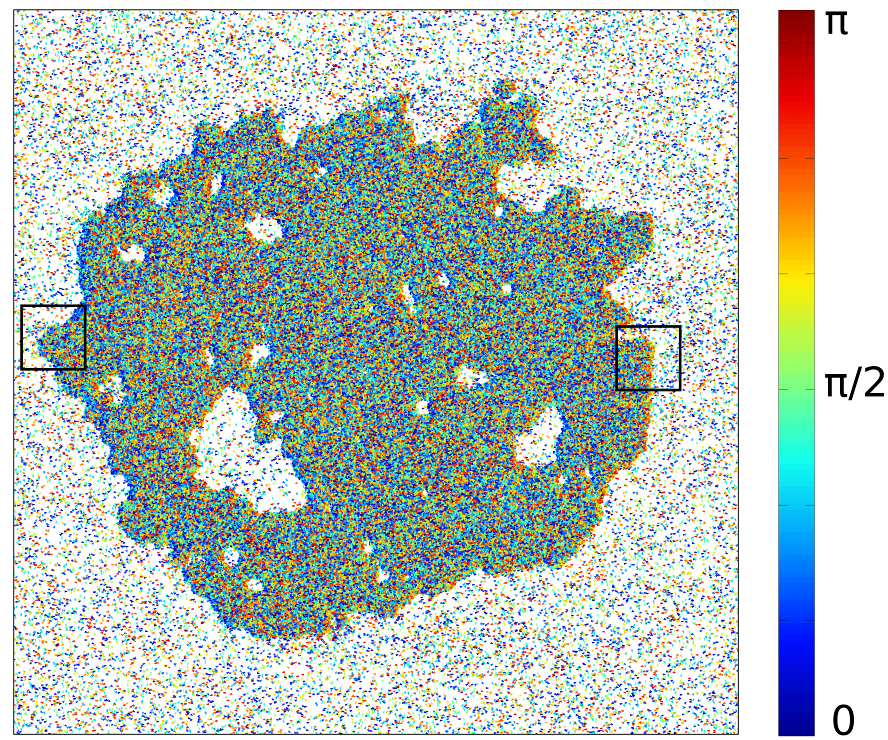

$\longrightarrow$ **blue 0** $\longleftarrow$ **red π**

The colours indicate the direction $\mathbf{n}_i$ along which the particles are pushed by the active force $f_{\rm act}$

MIPS - ABP

Identification via the local density distributions - dense & gas

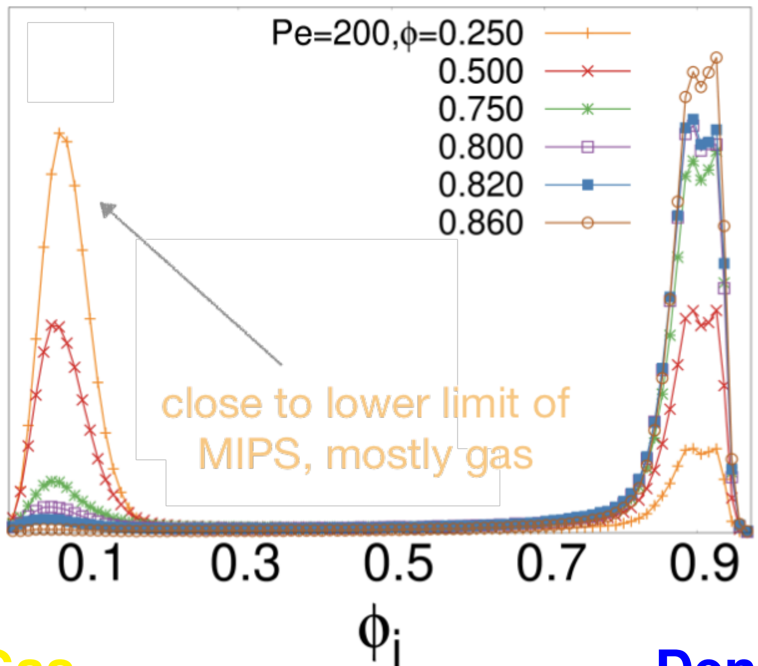

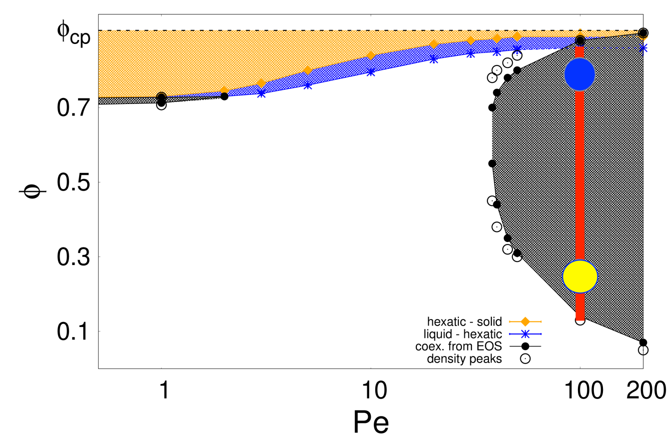

Gas **Dense**

The position of the peaks does not change while changing the global packing fraction ϕ but their relative height does. Transfer of mass from gas to **dense** component as ϕ increases

The Dense Phase - ABP

Hexatic patches, defects & bubbles in the stationary limit

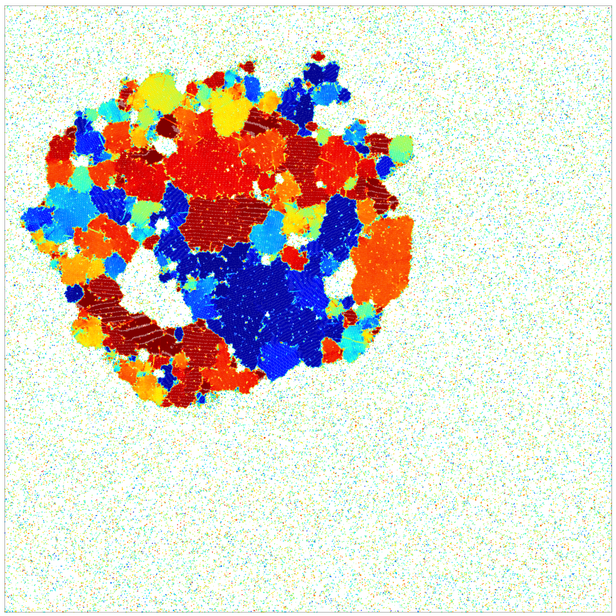

Dense/dilute separation[1]

For low packing fraction ϕ

a single round droplet

Growth[2] of clusters[3] with a mosaic

of hexatic orders[3] with

gas bubbles[2,4,5] & defects[6]

[1] Cates & Tailleur, Annu. Rev. Cond. Matt. Phys. 6, 219 (2015)

[2] Caporusso, Digregorio, Levis, LFC & Gonnella, PRL 125, 178004 (2020)

[3] Caporusso, LFC, Digregorio, Gonnella, Levis & Suma, PRL 131, 068201 (2023)

[4] Tjhung, Nardini & Cates, PRX 8, 031080 (2018)

[5] Shi, Fausti, Chaté, Nardini & Solon, PRL 125, 168001 (2020)

[6] Digregorio, Levis, LFC, Gonnella & Pagonabarraga, Soft Matter 18, 566 (2022)

The Coloured Patches - ABP

Local hexatic order parameter video

Orientational order

Local hexatic order parameter

$$\psi_{6j} = \frac{1}{nn_j} \sum_{k=1}^{nn_j} e^{i6\theta_{jk}}$$

nn_j nearest-neighbours of the Voronoi cell

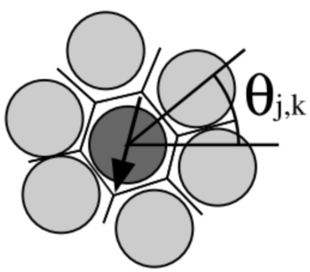

video

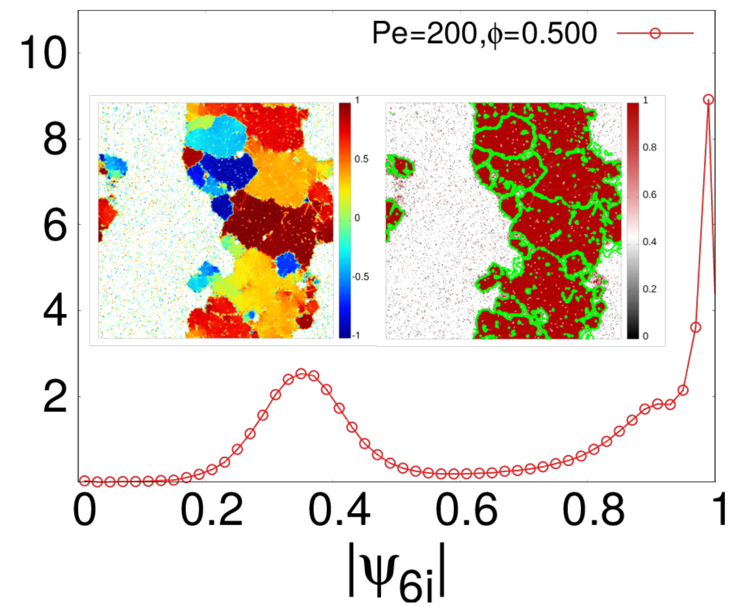

gas **dense**

in correspondence with the peaks

of the distribution of local densities

$$P(R_H) \sim e^{-R_H/R_H^*}$$

Interfaces

Macro vs micro - ABP

Stationary state - video

Local hexatic order map　　Local density map

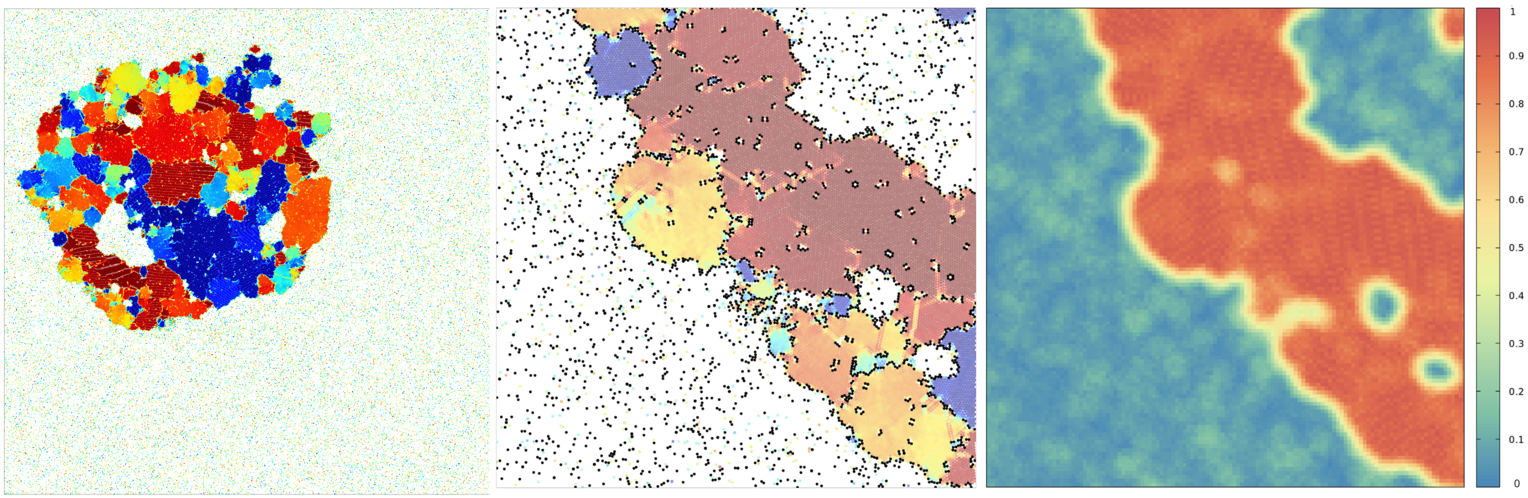

Local hexatic order saturates to a system size independent value

Defects on the boundaries between different hexatic ordered patches

Bubbles within the dense droplet

Interfaces - ABP

Strings of defects – along hexatic-hexatic interfaces

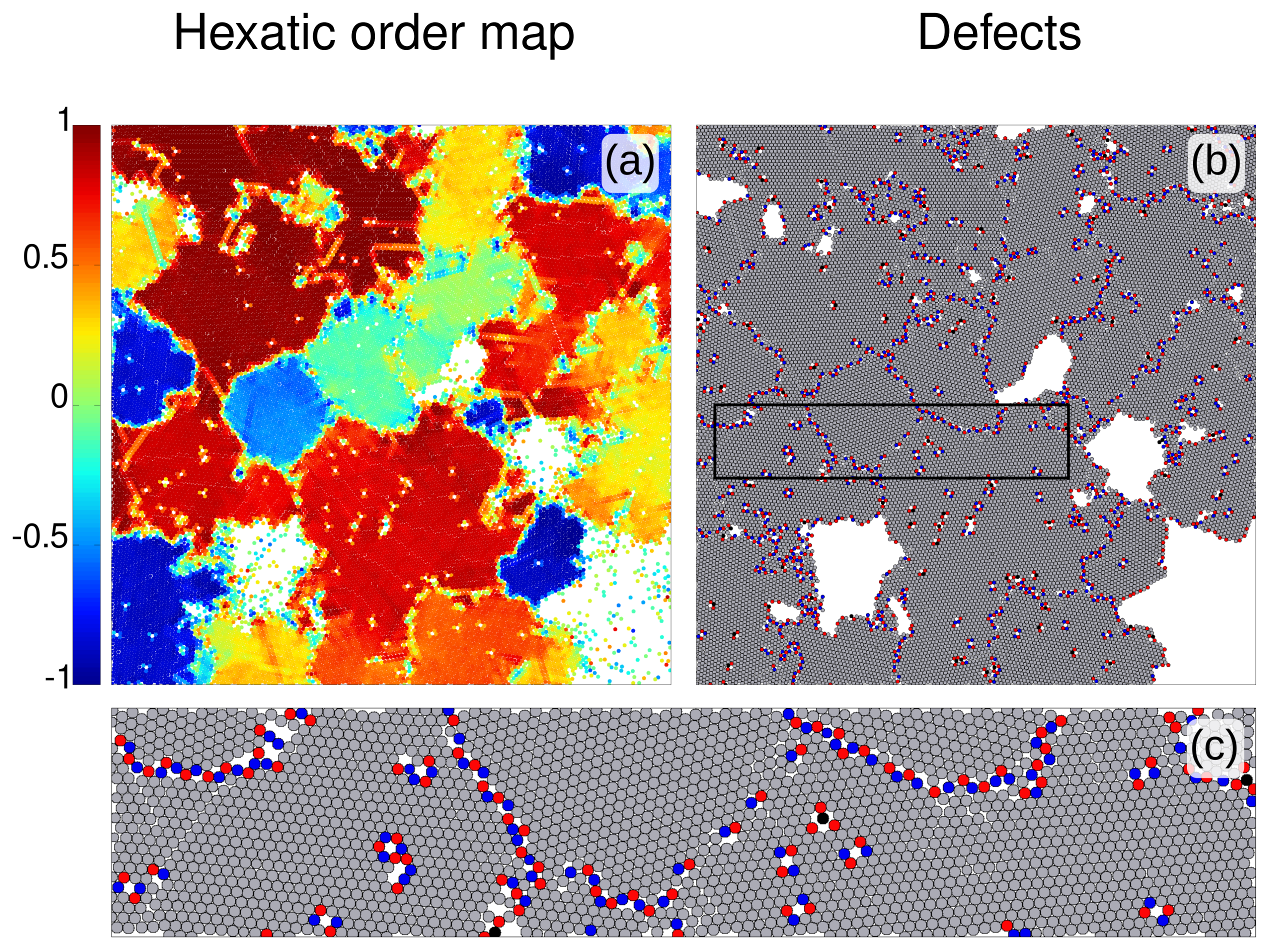

Zoom over the rectangular selection. Disks with **five** & **seven** neighbours

Clusters of defects - ABP

Size distribution - Finite size cut-off

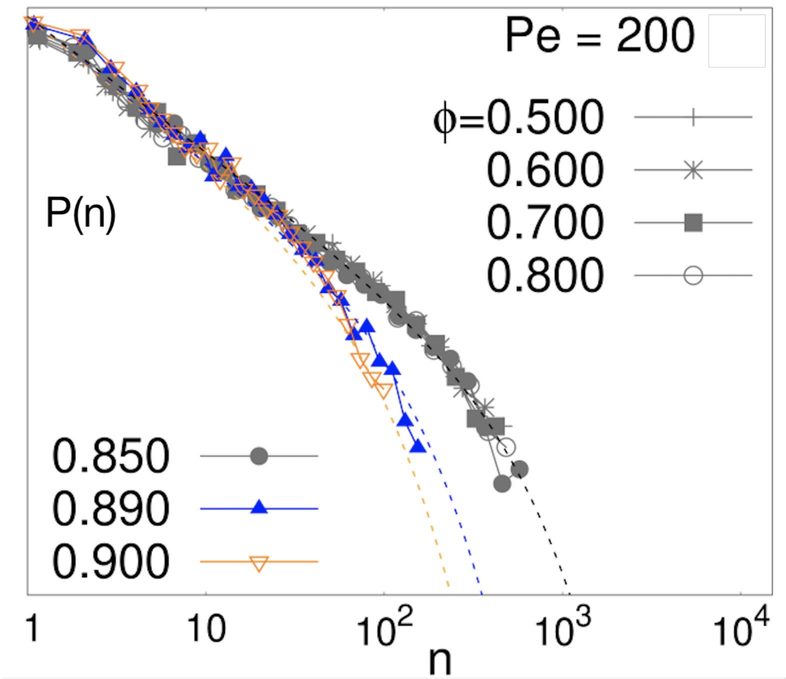

$$P(n) \simeq n^{-\tau} e^{-n/n^*}$$

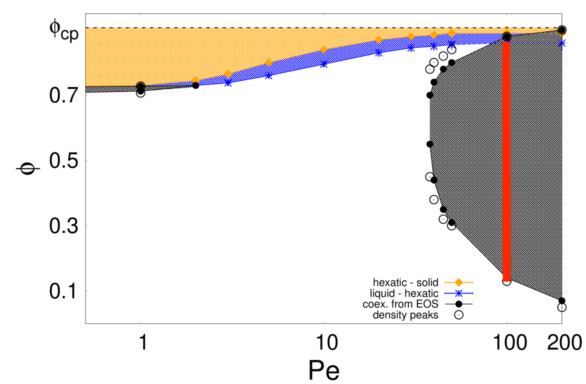

Independence of ϕ at fixed Pe within MIPS

$n^* \sim 30, 50, 200$ in the **solid**, **hexatic** and **MIPS**, respectively, and $\tau \sim 2.2$

No percolation, interrupted by the bubbles

Bubbles in Cavitation - ABP

At the interfaces between coloured patches bubbles pop up

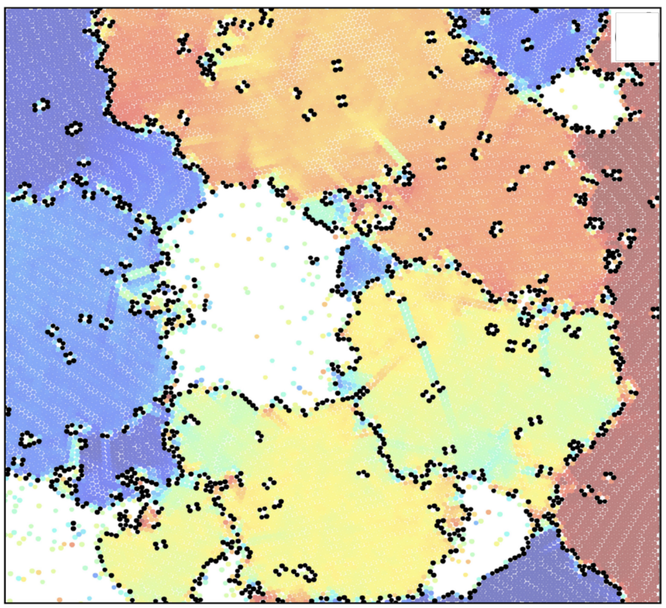

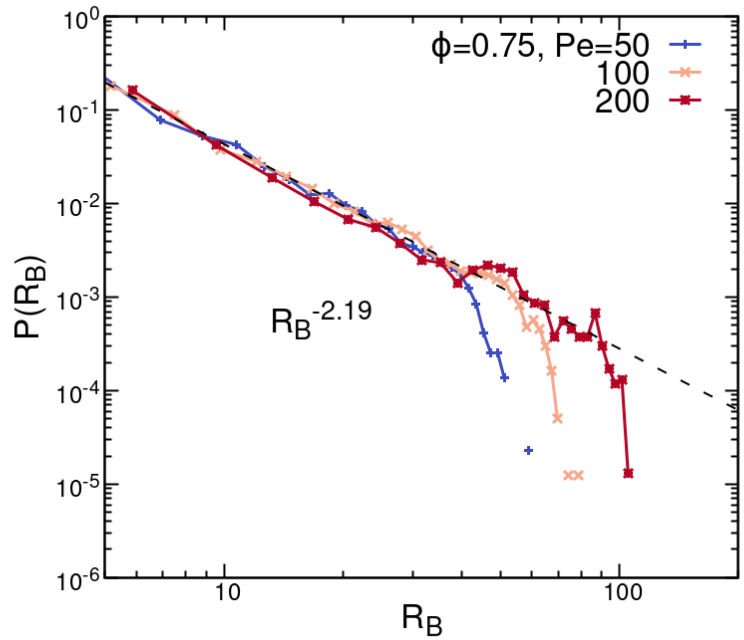

Bubbles appear and disappear at the interfaces between hexatic patches

Algebraic distribution of bubble sizes with a Pe-dependent exponential cut-off

Active Brownian Matter

Table with results

	Disks	Dumbbells
Non-eq Steady-State	$R \sim aL$ $R_H \sim R_H^* \ll L$ $P(R_B) \sim R_B^{-\tau} e^{-\frac{R_B}{R_B^*}}$	
Approach to NESS	**Next**	

Dynamic Structure Factor - ABP

Growing length of dense component

I peak:
system average size

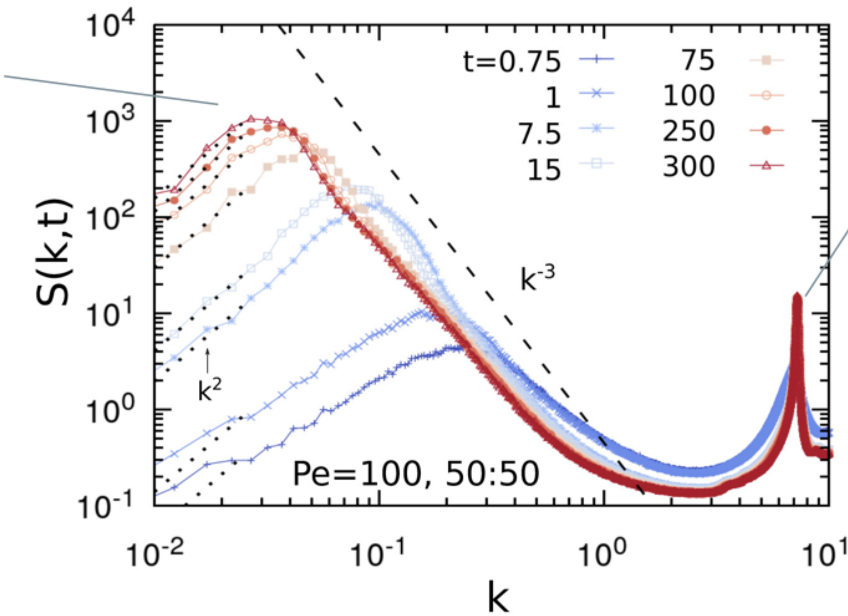

II peak:
particles' packing

$$S(\mathbf{k},t) = \sum_{i=1}^{N} e^{i\mathbf{k}(\mathbf{r_i}-\mathbf{r_j})}$$

related to Fourier transform of the pair correlation function

$$k_{\mathrm{I}}(t) \propto R^{-1}(t)$$

No sign of fractality here. Porod's law $S(k) \sim k^{-(d+1)}$ for compact domains with sharp interfaces

The Growth Law - ABP

Growing length of the dense component and regimes

Different Pe

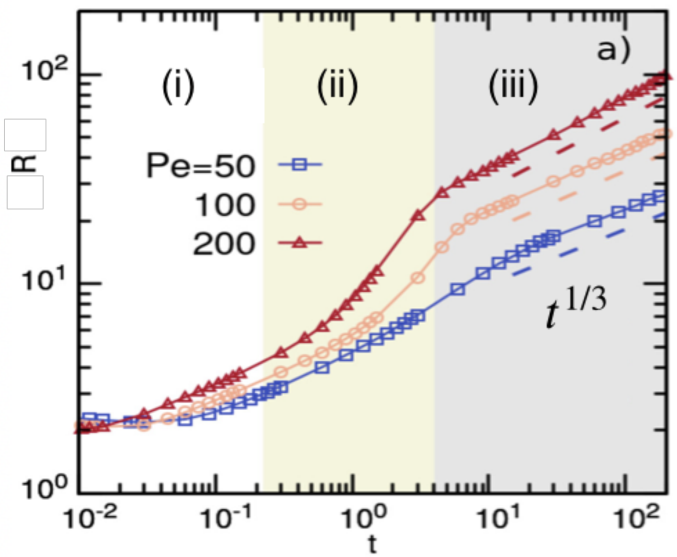

Movie

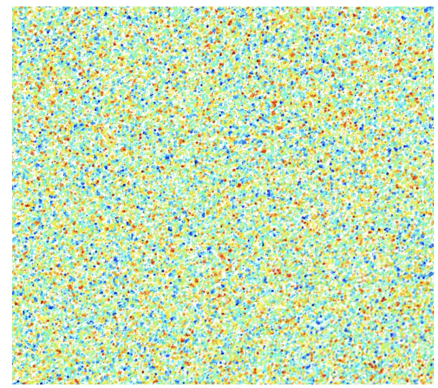

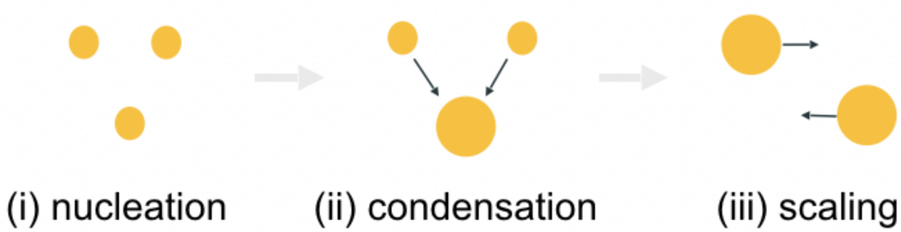

$R(t) \sim t^{1/3}$ for all Pe

Lifshitz-Slyozov-Wagner

In scaling regime $t^{1/3}$ like in passive scalar phase separation.

Redner, Hagan & Baskaran, PRL 110, 055701 (2013). Stenhammar et al., Soft Matter 10, 1489 (2014)

Local Hexatic Order - ABP

Growing length of the orientational order – regimes

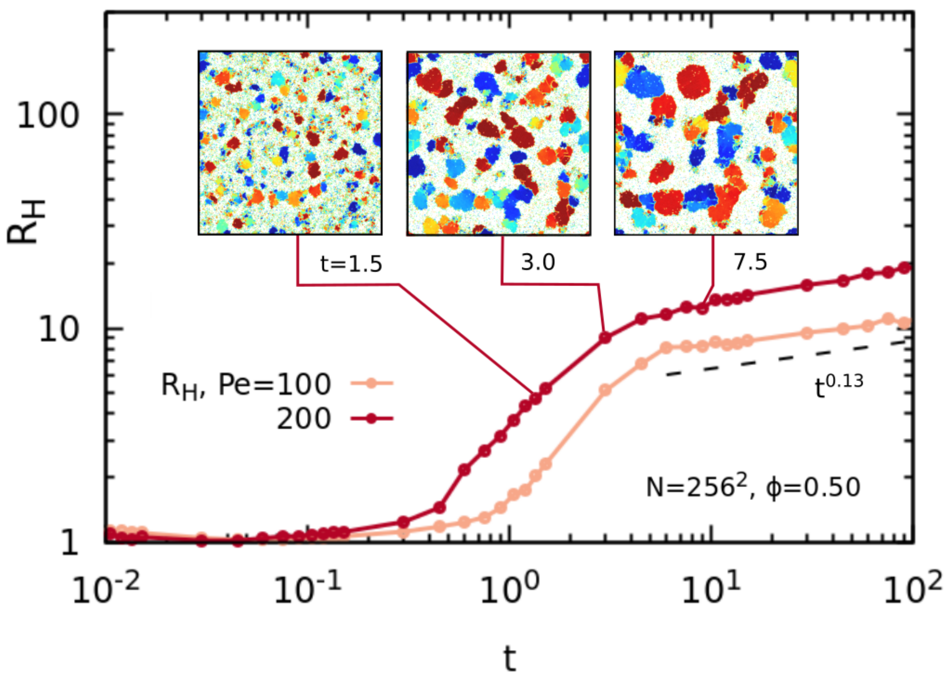

Local hexatic order parameter

$$\psi_{6j} = \frac{1}{nn_j} \sum_{k=1}^{nn_j} e^{i6\theta_{jk}}$$

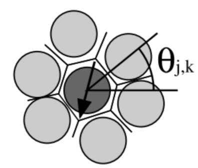

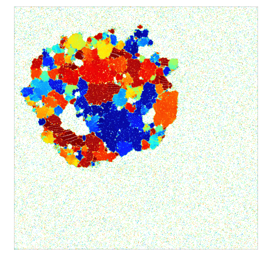

Full hexatically ordered small clusters

Larger clusters with several orientational order within

$R_H \sim t^{0.13}$ in the scaling regime and $R_H \to R_H^* \ll L$

Similar to pattern formation, e.g.

Vega, Harrison, Angelescu, Trawick, Huse, Chaikin & Register, PRE 71, 061803 (2005)

Macro vs. Micro - ABP

Dense phase vs. hexatic growth

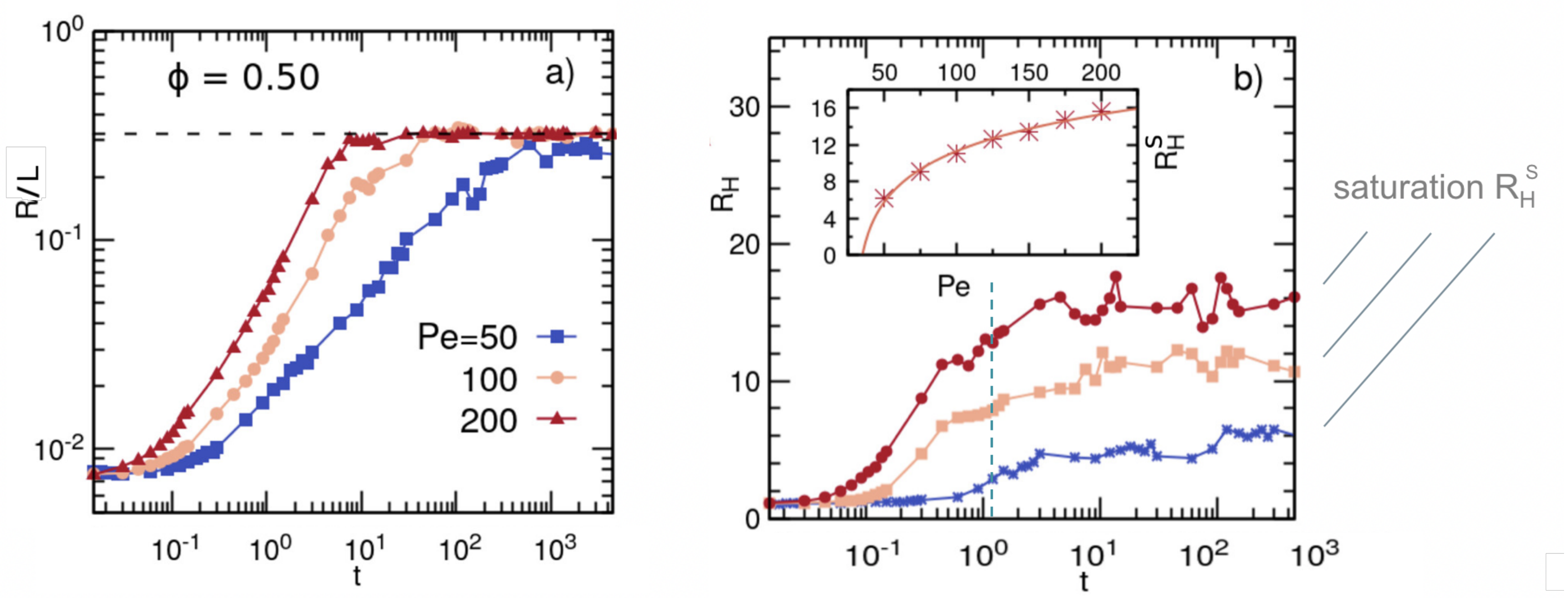

$R(t) \to aL$ $\qquad$ $R_H(t) \to R_H^*$ finite $\qquad$ $R_H^* \nearrow$ Pe $\nearrow$

Active Brownian Matter

Table with results

	Disks	Dumbbells
Non-eq Steady-State	$R \sim aL$ $R_H \sim R_H^* \ll L$ $P(R_B) \sim R_B^{-\tau} e^{-\frac{R_B}{R_B^*}}$	
Approach to NESS	$R \sim t^{1/3} \to aL$ $R_H \sim t^{0.13} \to R_H^*$	

Mechanism

Two (non-exclusive) possibilities

1. Is it like the one of **passive attractive particles** ?

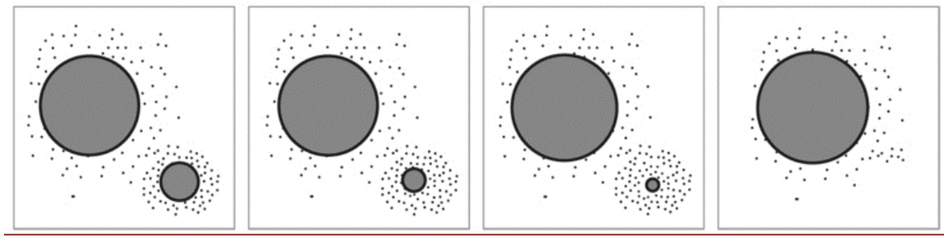

Ostwald ripening

2. Are there other **processes** at work in the active case ?

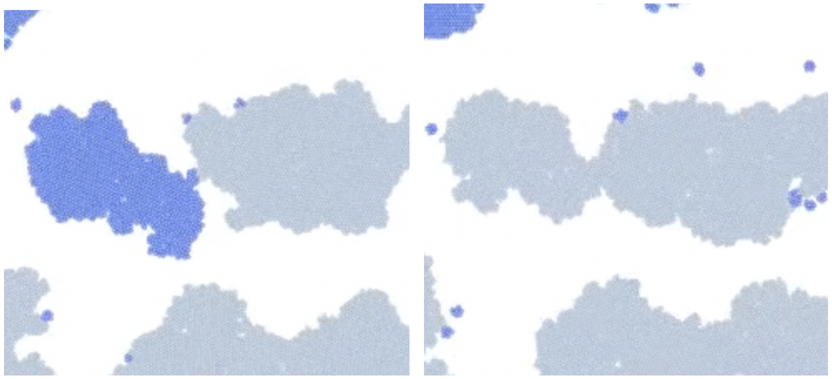

Cluster-cluster aggregation

Dense Clusters - ABP

Instantaneous configurations (DBSCAN)

Passive - attractive

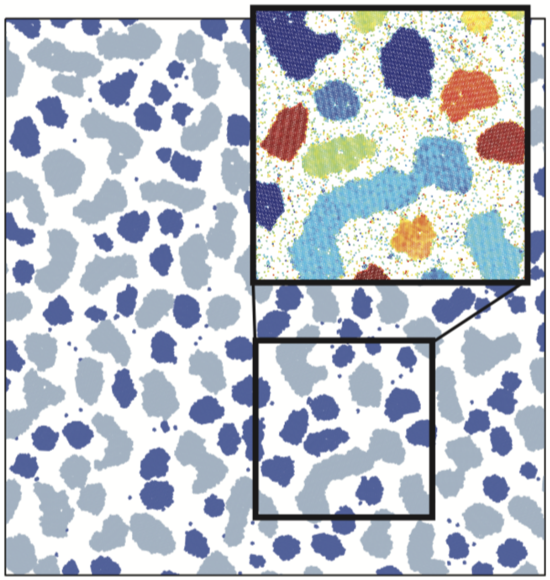

Active - repulsive

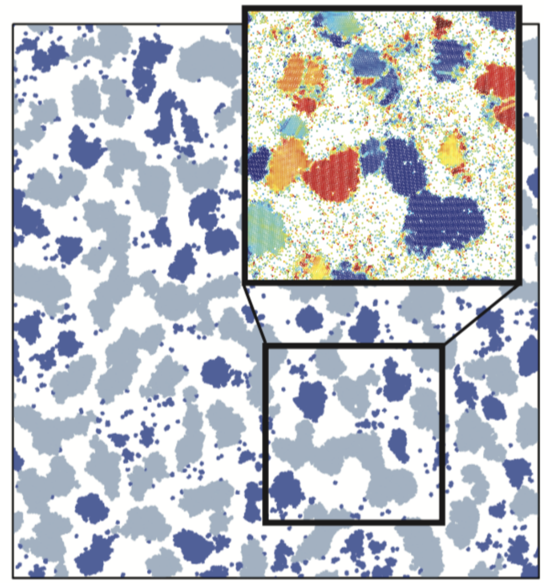

The Mie potential is not truncated in the passive case $\Rightarrow$ attractive

Parameters are such that $R(t)$ is the same in the two systems

Colors in the zoomed box indicate orientational order

Caporusso, LFC, Digregorio, Gonnella, Levis & Suma, PRL 131, 068201 (2023)

Dense Clusters - ABP

Visual facts about the instantaneous configurations

Similarities

- Large variety of shapes and sizes (masses)

  Co-existence of

  small regular (**dark blue**) and large elongated (**gray**) clusters

Differences

- Rougher interfaces in active
- Homogeneous (passive) vs. heterogeneous (active) orientational order within the clusters

Clusters' Dynamics - ABP

Tracking of individual cluster motion - video

Active

Passive

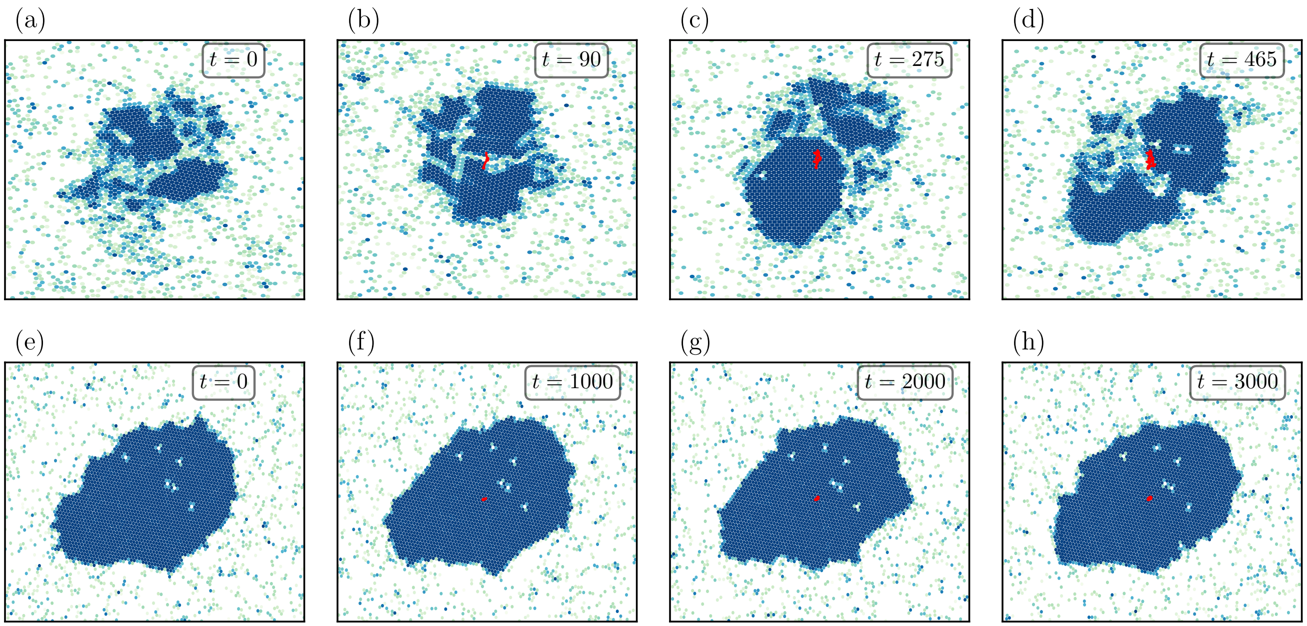

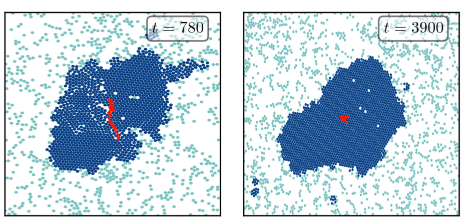

In **red** the center of mass trajectory

Active is much faster than passive

Dense Clusters - ABP

Visual facts about the cluster dynamics

In both cases, **Ostwald ripening** features

- small clusters evaporate
- gas particles attach to large clusters

In the **active system**

- clusters displace much more & sometimes aggregate
- they also break & recombine

like in **diffusion limited cluster-cluster aggregation**

Clusters' Diffusion - ABP

Mean Square Displacement

Average over all clusters **Mass dependence**

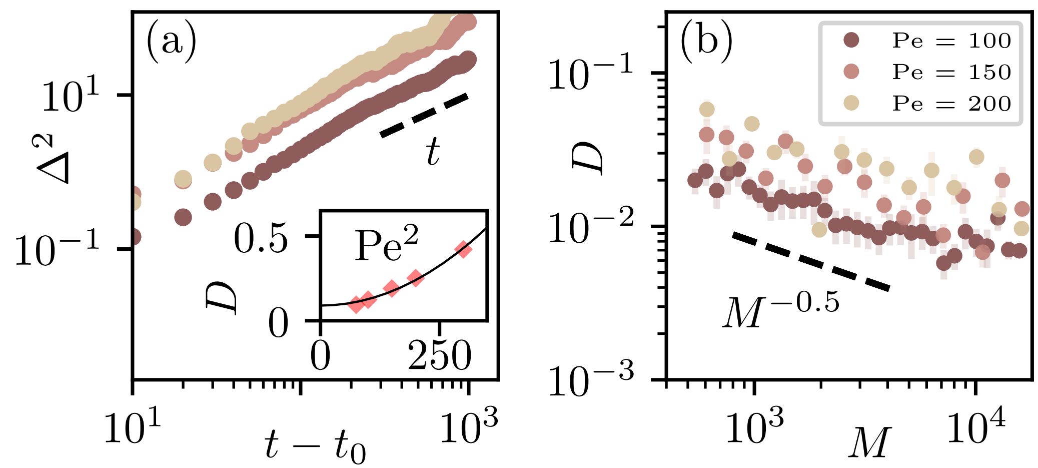

$$\Delta_k^2(t,t_0) = [\mathbf{r}^{(k)}_{\mathrm{c.o.m.}}(t) - \mathbf{r}^{(k)}_{\mathrm{c.o.m.}}(t_0)]^2 \sim 2d\, D(M_k, \mathrm{Pe})\,(t-t_0)$$

A sum of random forces yields $D \sim M^{-1}$

Passive tracer in a dilute active bath $D \sim R^{-1} \sim M^{-1/2}$ **Solon & Horowitz (22)**

Passive & very heavy isolated active clusters $D \sim M^{-1}$

Clusters' Geometry - ABP

Scatter plots: small regular – large fractal

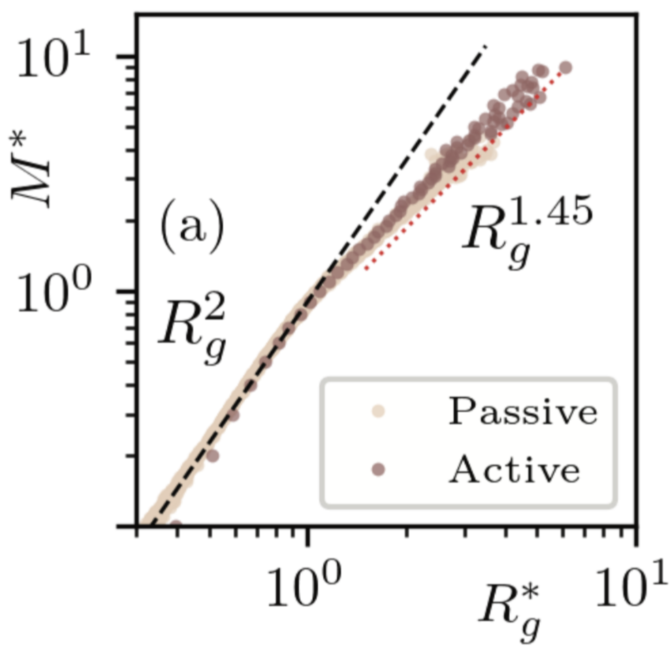

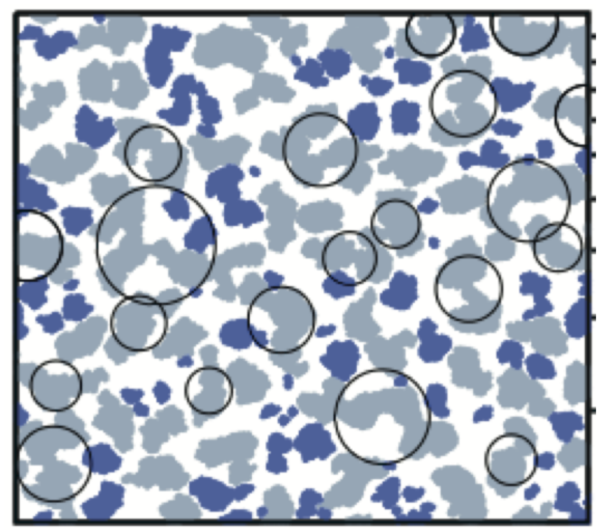

Cluster mass $M_k^*(t) = \frac{M_k(t)}{\overline{M}(t)}$ Gyration radius $R_{g\,k}^*(t) = \frac{R_{g\,k}(t)}{\overline{R_g}(t)}$

Data sampled in the scaling regime $t = 10^3 - 10^5$ every 10^3 time steps

$\overline{O}(t) = \frac{1}{N_c(t)} \sum_{k=1}^{N_c(t)} O_k(t)$ and $N_c(t)$ the total number of clusters at time t

Cluster-Cluster Aggregation

Smoluchowski argument

From $\overline{R}_g \sim t^{1/z}$ and using $D(M) \sim M^{-\alpha}$

Smoluchowski eq. $\Rightarrow z = d_f(1+\alpha) - (d - d_w)$

Regular clusters $M_k < \overline{M}$

$d_f = d = d_w = 2$

$\alpha = 0.5$

$z = 2(1+0.5) = 3$

Fractal clusters $M_k > \overline{M}$

$d_f = 1.45, d = 2$ and $d_w \sim 2$

$\alpha = 0.5$ in the bulk

$z = 1.45(1+0.5) = 2.18 < 3$

Reviews on the application of fractals to colloidal aggregation

R. Jullien, Croatia Chemica Acta 65, 215 (1992) P. Meakin, Physica Scripta 46, 295 (1992)

Regular vs Fractal Clusters

Radius of gyration and number of ABP clusters

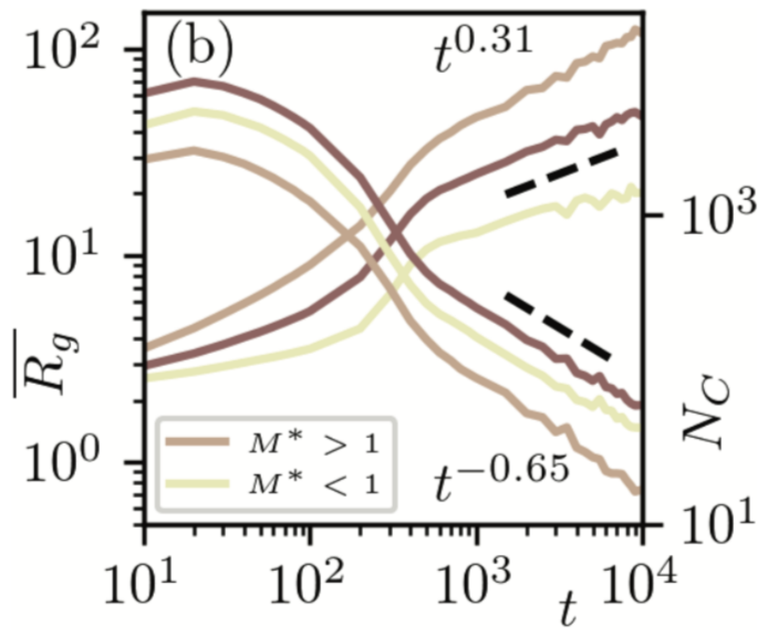

regular $z \gtrsim 3$

More

Dominate

fractal $z < 3$

Less

average $z = {}^1\!/_{0.31} \sim 3$

All

Active Brownian Matter

Table with results

	Disks	Dumbbells
Non-eq Steady-State	$R \sim aL$ $R_H \sim R_H^* \ll L$ $P(R_B) \sim R_B^{-\tau} e^{-\frac{R_B}{R_B^*}}$	**Next**
Approach to NESS	$R \sim t^{1/3}$ $R_H \sim t^{0.13}$ Ostwald ripening & Cluster-cluster aggregation	**Next**

Active Brownian Dumbbells

e.g., a diatomic molecule or a dumbbell

Two spherical atoms with diameter σ and mass m

Massless spring modelled by a finite extensible non-linear elastic (fene) force between the atoms $\mathbf{f}_{\text{fene}} = -\dfrac{k(\mathbf{r}_i - \mathbf{r}_j)}{1 - r_{ij}^2/r_0^2}$ with an additional repulsive contribution (WCA potential) to avoid atomic/colloidal overlapping (see next slides)

Langevin modelling of the interaction with the embedding fluid:

isotropic viscous forces, $-\gamma\dot{\mathbf{r}}_i$, and independent noises, $\boldsymbol{\xi}_i$, on the beads.

Translational motion (centre of mass)

Rotations due to effective torque applied by noise

Vibrations due to the fene potential (frozen)

Active Brownian Dumbbells

a dumbbell made of a colloid 1 and a colloid 2

$$\begin{aligned} m\ddot{\mathbf{r}}_1 + \gamma\dot{\mathbf{r}}_1 &= \mathbf{f}_{\text{pot}_1}(\mathbf{r}_1, \mathbf{r}_2) + \mathbf{f}_{\text{act}} + \boldsymbol{\xi}_1 \\ m\ddot{\mathbf{r}}_2 + \gamma\dot{\mathbf{r}}_2 &= \mathbf{f}_{\text{pot}_2}(\mathbf{r}_1, \mathbf{r}_2) + \mathbf{f}_{\text{act}} + \boldsymbol{\xi}_2 \end{aligned}$$

with $\mathbf{f}_{\text{pot}} = \mathbf{f}_{\text{wca}} + \mathbf{f}_{\text{fene}}$, $V = V_{\text{wca}} + V_{\text{fene}}$ and

$\boldsymbol{\xi}_i$ independent Gaussian thermal noises acting on the two beads,

zero average $\langle \xi_a^i(t) \rangle = 0$ and $\langle \xi_a^i(t) \xi_b^j(t') \rangle = 2\,\gamma k_B T\, \delta_{ij}\delta_{ab}\, \delta(t-t')$

$i, j = 1, 2$ bead labels, $a, b = 1, \ldots, d$ coordinate labels

Phase Diagram - ABD

cfr. ABPs, plenty of interesting differences

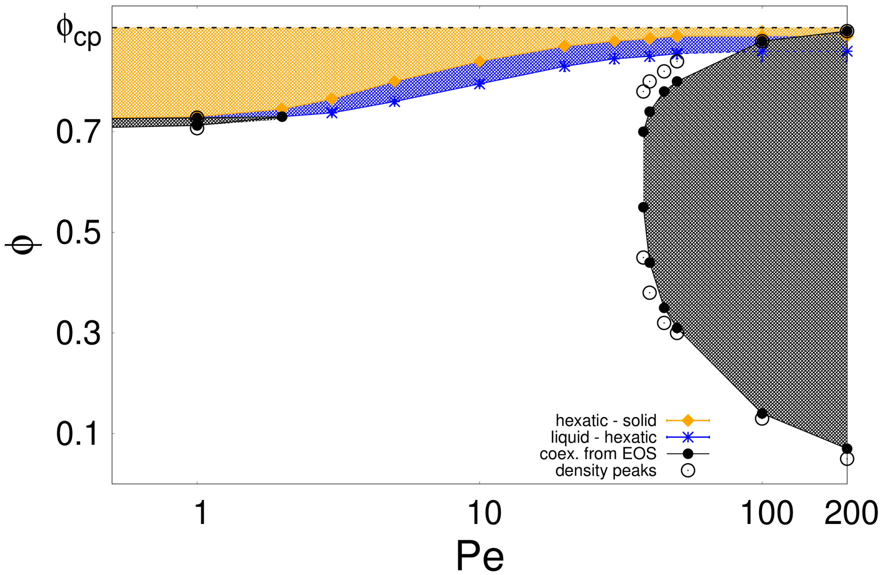

AB Disks

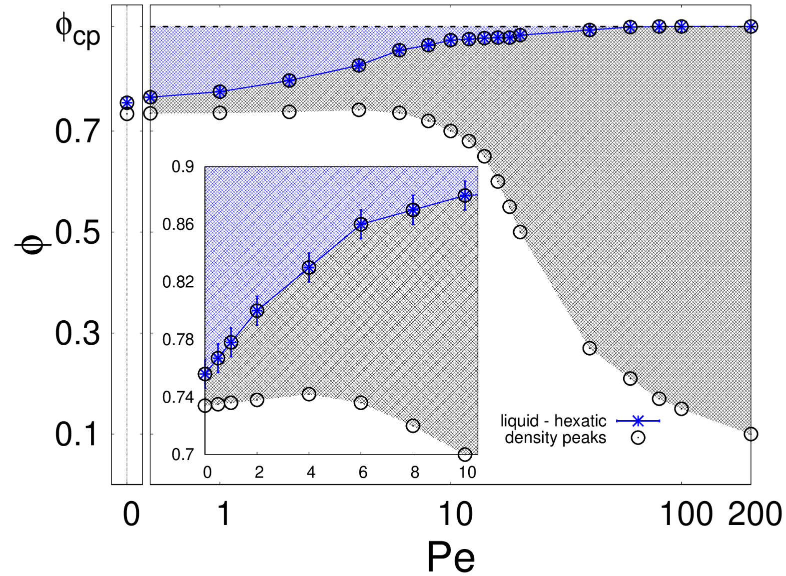

AB Dumbbells

LFC, Digregorio, Gonnella & Suma, Phys. Rev. Lett. 119, 268002 (2017)

Growth of Dense Phase - ABD

ABP vs ABD both at Pe = 100 and 50 : 50

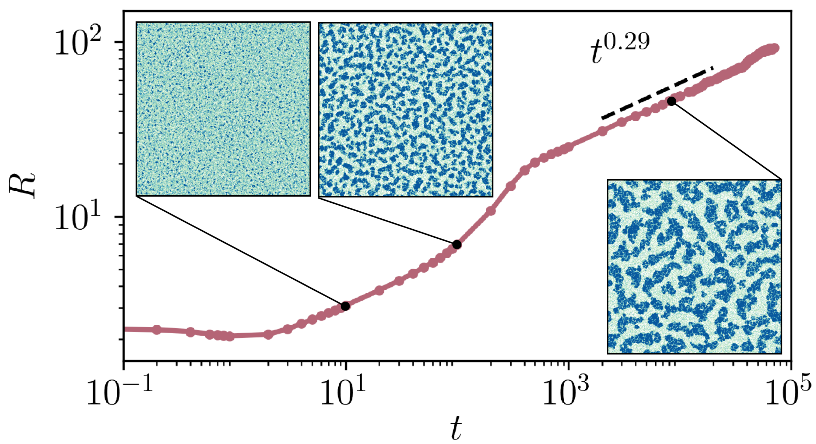

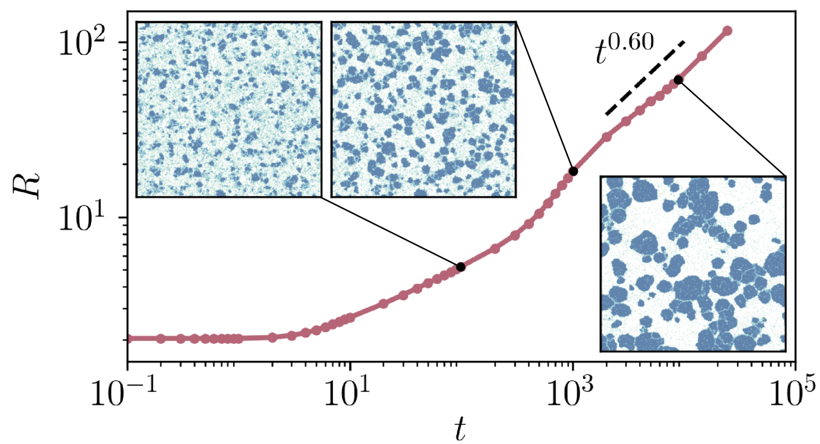

AB Disks

slower

$t^{0.3}$

AB Dumbbells

faster

$t^{0.6}$

Caporusso, LFC, Digregorio, Gonnella & Suma, Soft Matter 20, 4208 (2024)

Local Hexatic Order - ABD

Growth towards saturation

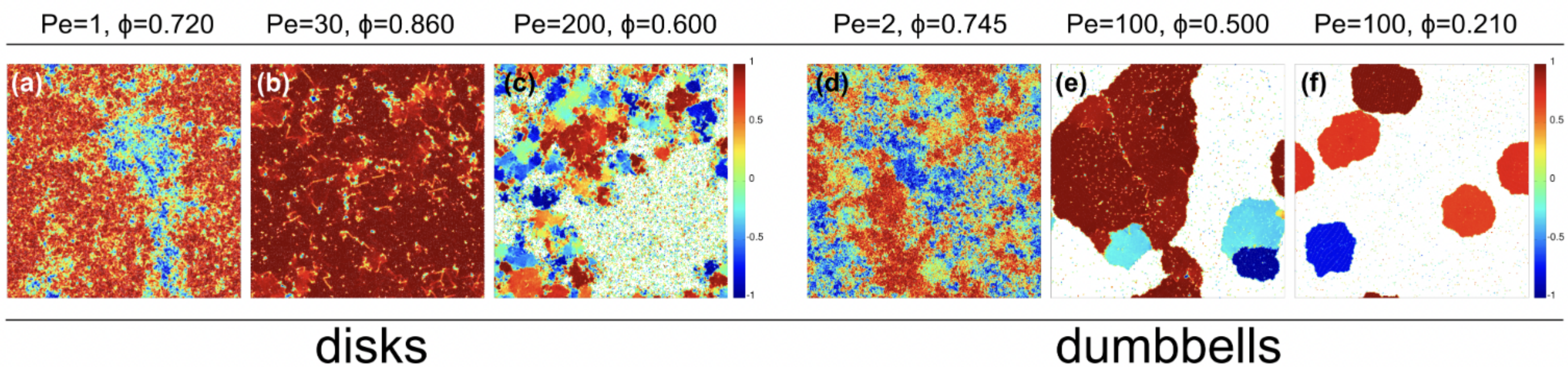

Video

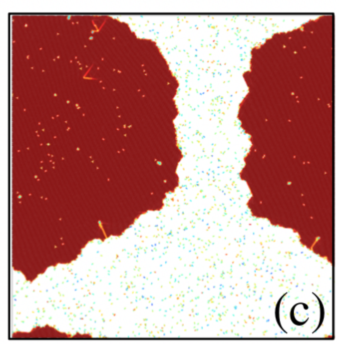

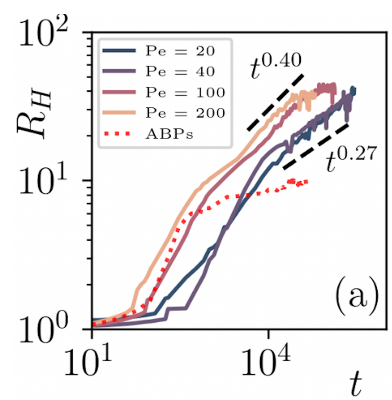

$$R_H \sim t^{0.3} \to R$$

Faster growth than for ABPs, full orientational order is reached & no bubbles

Caporusso, LFC, Digregorio, Gonnella & Suma, Soft Matter 20, 4208 (2024)

Isolated Dumbbell Clusters

Motion

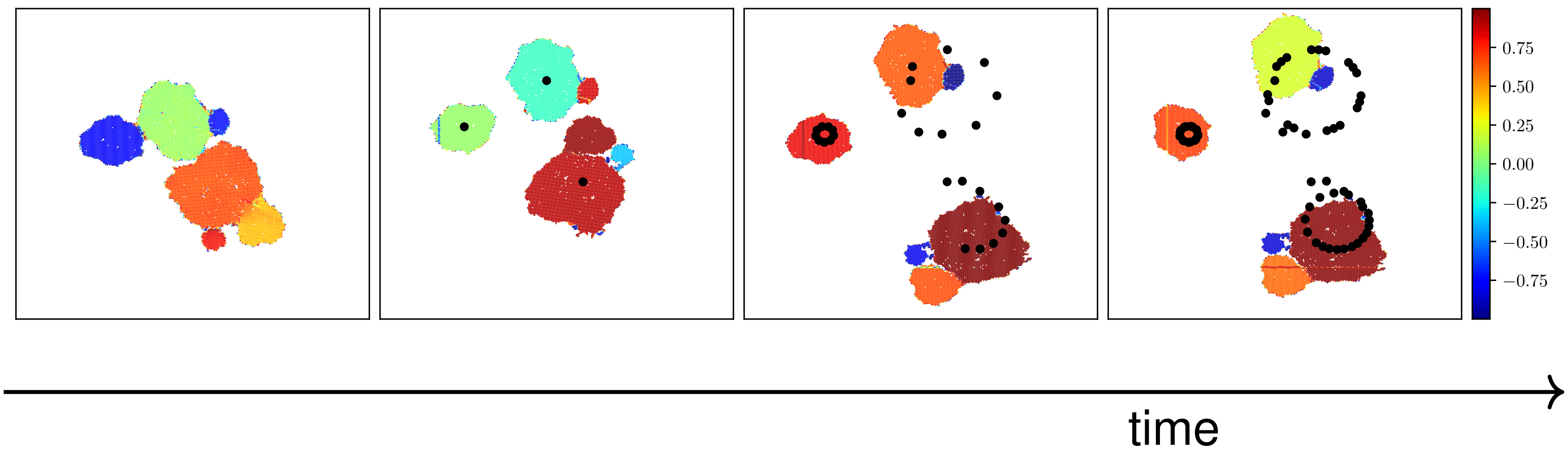

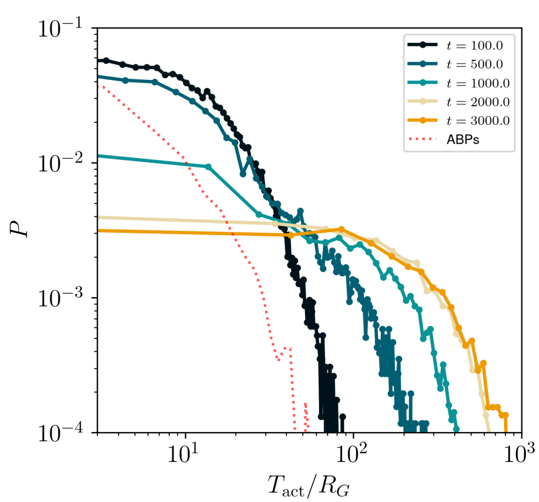

- Instability of clusters with multi-orientational order : they break up along the hexatic interfaces
- The center of mass (c.o.m.) of each cluster α rotates with constant angular velocity ω_α
- The clusters rotate around their c.o.m. with the same angular velocity ω_α

Torque

Solid body motion

Isolated Dumbbell Clusters

Motion video

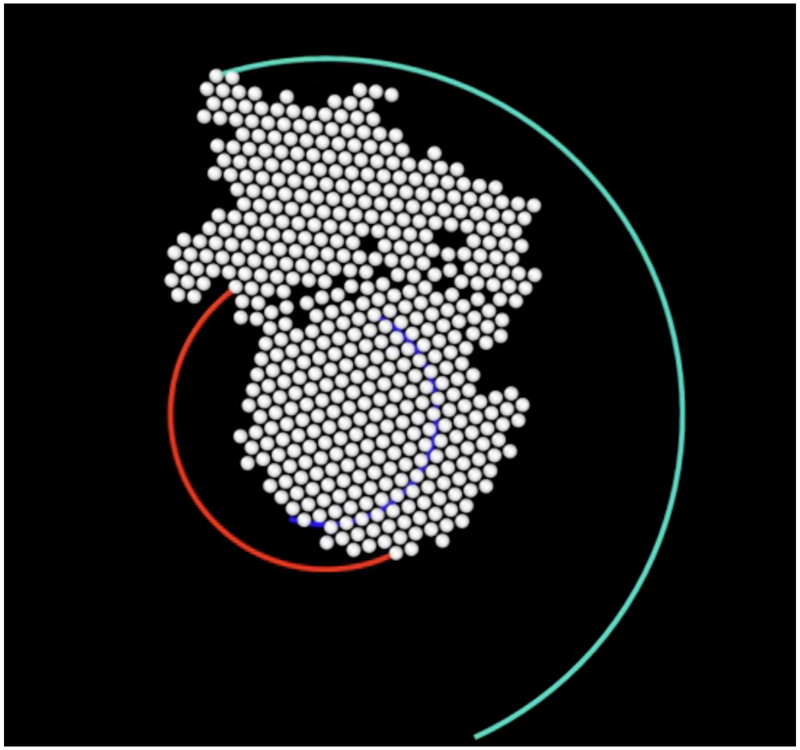

Four clusters with different mass

under three active forces each

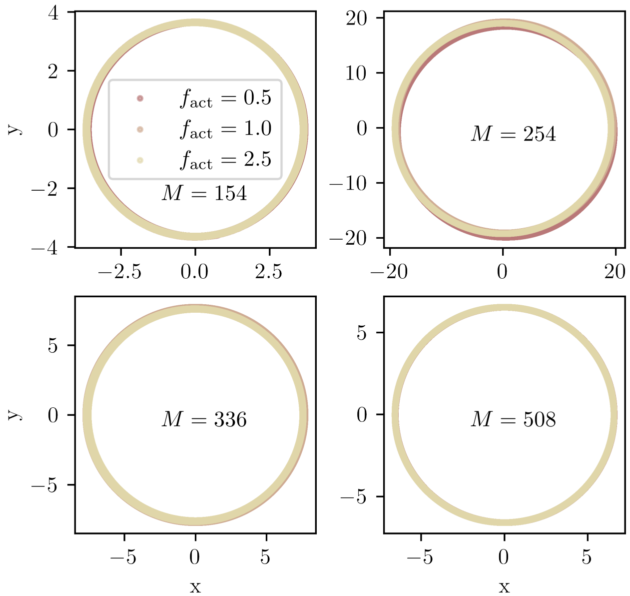

Model

Solid body motion

$$M\ddot{\mathbf{R}}_{\rm cm} = \mathbf{F}_{\rm drag} + \mathbf{F}_{\rm act}$$ (with $\mathbf{F}_{\rm act} = \sum_{i\in C} \mathbf{f}_{{\rm act}\,i}$ and $\mathbf{F}_{\rm drag} = -\gamma \frac{M}{m} \dot{\mathbf{R}}_{\rm cm}$)

$$\dot{\mathbf{L}} = \mathbf{T}_{\rm drag} + \mathbf{T}_{\rm act}$$ with

$$\left.\begin{array}{r} \mathbf{L} \\ \mathbf{T}_{\rm drag} \\ \mathbf{T}_{\rm act} \end{array}\right\} = \sum_{i\in C} (\mathbf{r}_i - \mathbf{R}_{\rm cm}) \times \left\{\begin{array}{l} m\,\frac{d}{dt}(\mathbf{r}_i - \mathbf{R}_{\rm cm}) \\ -\gamma\,\frac{d}{dt}(\mathbf{r}_i - \mathbf{R}_{\rm cm}) = -\frac{\gamma}{m}\,\mathbf{L} \\ \mathbf{f}_{{\rm act}\,i} \end{array}\right.$$

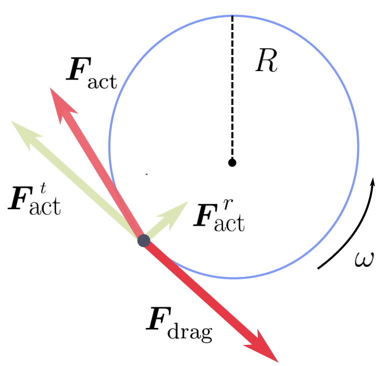

Sketch of forces acting on

the c.o.m. of the cluster

ω angular velocity

How does $R = R_{\rm cm}$ depend on $M, R_g, f_{\rm act}$?

Model

Circular motion

Overdamped approximation for angular momentum

$$\dot{\mathbf{L}} = \mathbf{T}_{\rm act} + \mathbf{T}_{\rm drag} \approx 0 \quad \Longrightarrow \quad \mathbf{T}_{\rm act} - {}^{\gamma}\!/_{m}\, \mathbf{L} \approx \mathbf{0} \quad \Longrightarrow \quad L \approx \frac{m}{\gamma}\, T_{\rm act}$$

Using now $L = I\omega = MR_g^2\,\omega$ in the last equation $\boxed{\omega \approx \dfrac{m}{M}\,\dfrac{T_{\rm act}}{\gamma R_g^2}}$

On the other hand the balance of the tangential forces yields

$$F^t_{\rm act} = F_{\rm drag} = \left({}^{M}\!/_{m}\right)\gamma \dot{R}_{\rm cm} \approx \left({}^{M}\!/_{m}\right)\gamma\omega R \quad \Longrightarrow \quad \boxed{R = \frac{m}{M}\,\frac{F^t_{\rm act}}{\gamma}\,\frac{1}{\omega}}$$

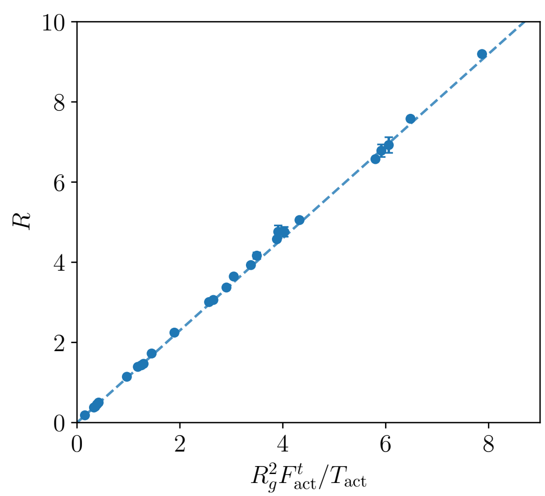

Putting these two equations together

$\leftarrow$ Test $\boxed{R = R_g^2 \underbrace{\dfrac{F^t_{\rm act}}{T_{\rm act}}}_{\text{independent of } f_{\rm act}}}$

Trajectories

Circular

$$\boxed{R = M R_g \frac{F^r_{\rm act}}{T_{\rm act}}}$$

The radius of each c.o.m. trajectory

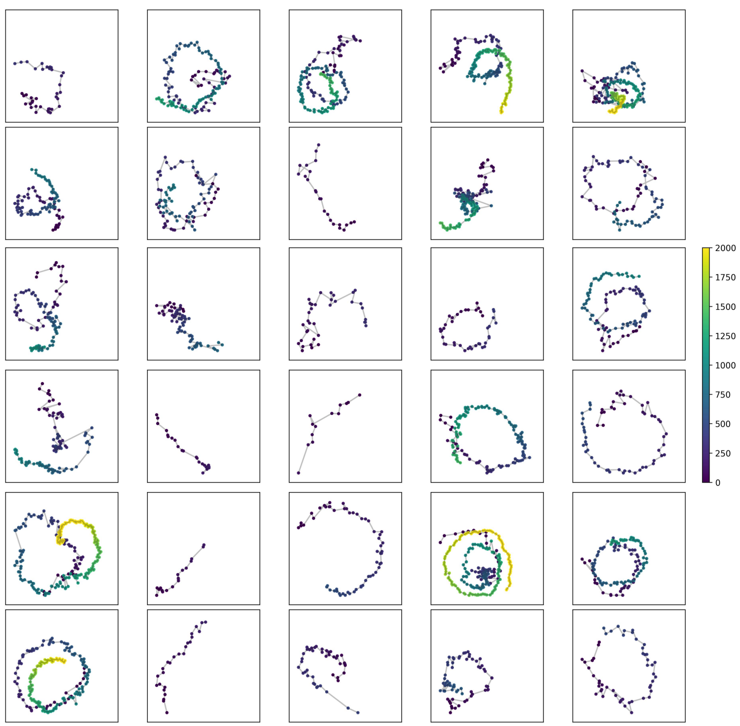

Trajectories in the bulk

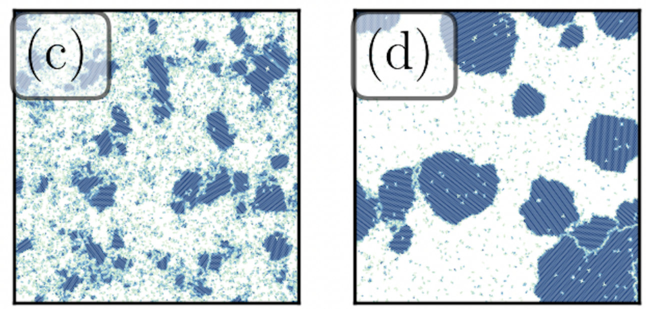

Non-vanishing:
active torque $\mathbf{T}_{\rm act}$ & force $\mathbf{F}_{\rm act}$
acting on the clusters

Rotation instead of ABP diffusion

Video

Caporusso, LFC, Digregorio, Gonnella & Suma, Soft Matter 20, 4208 (2024)

Active Brownian Matter

Table with results

	Disks	Dumbbells
Non-eq Steady-State	$R \sim L$ $R_H \sim R_H^* \ll L$ $P(R_B) \sim R_B^{-\tau} e^{-\frac{R_B}{R_B^*}}$	$R \sim R_H \sim L$
Approach to NESS	$R \sim t^{1/3} \to L$ $R_H \sim t^{0.13} \to R_H^*$ Ostwald ripening & Cluster-cluster aggregation	$R \sim t^{2/3} \to L$ $R \sim t^{0.3} \to L$ Rotation, breaking merging

ABPs vs ABDs

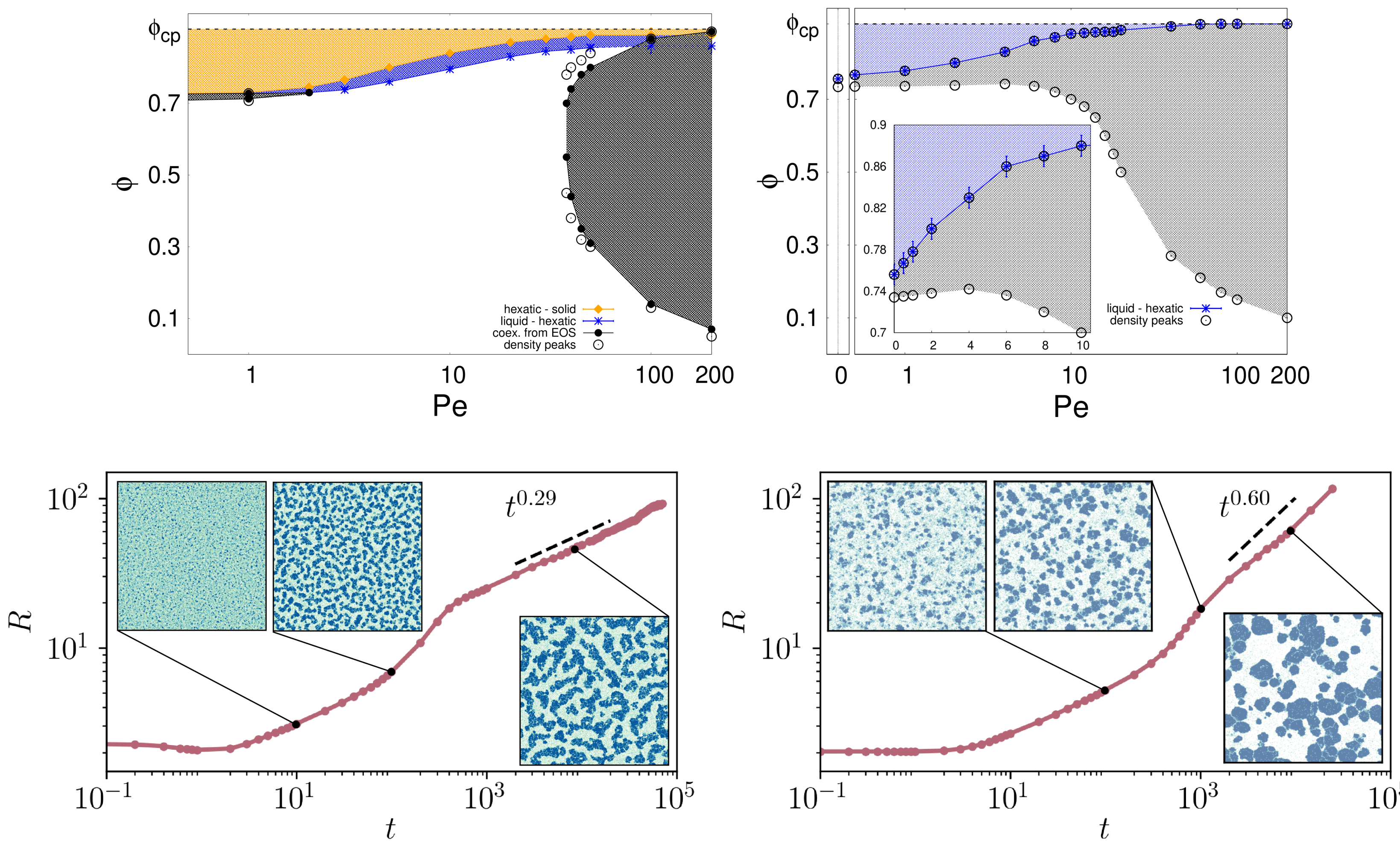

AB Disks

Cluster diffusion

AB Dumbbells

Cluster rotation

Extras

ABPs vs. ABDs

Hexatic order & Correlations

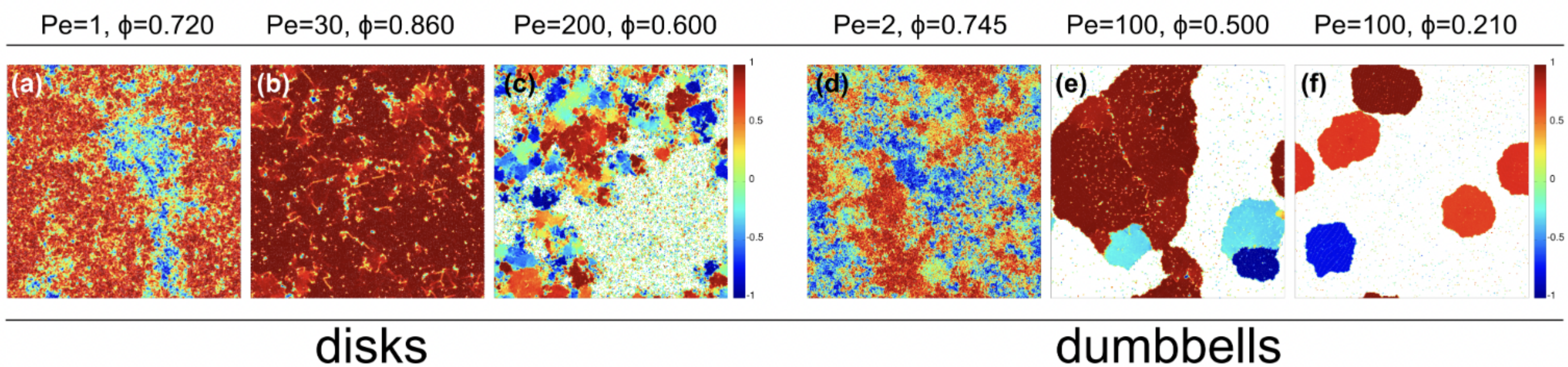

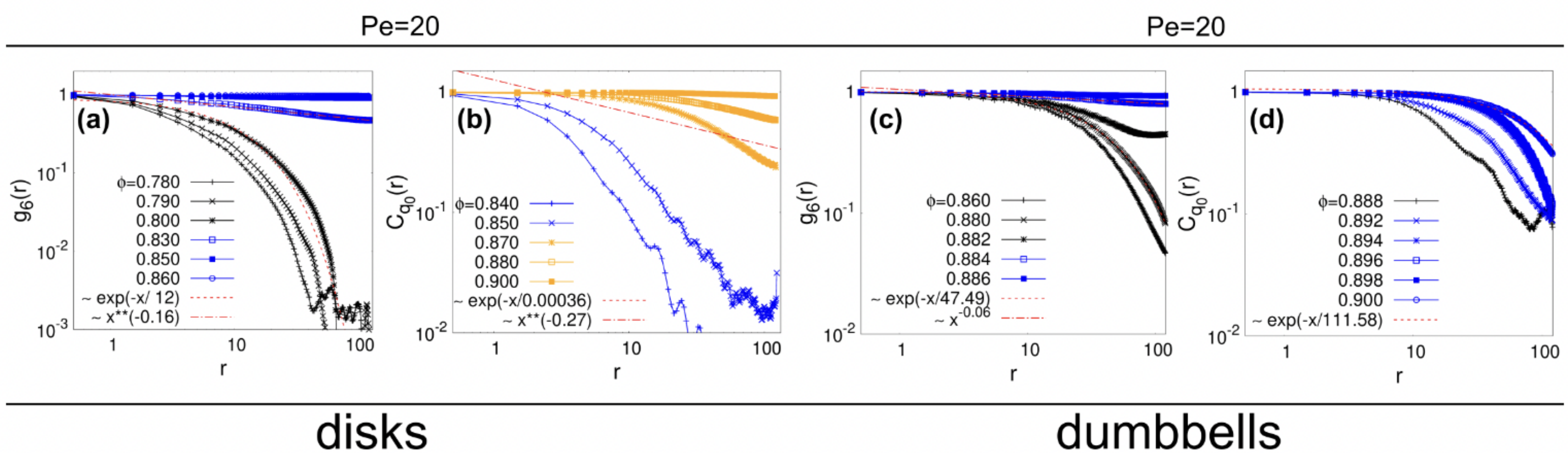

Digregorio, Levis, Suma, LFC, Gonnella, Pagonabarraga, J. Phys. C : Conf. Ser. 1163, 012073 (2019)

Cluster-cluster aggregation

Extended Smoluchowski argument

From $\overline{R}_g \sim t^{1/z}$ and using $D(M) \sim M^{-\alpha}$

Smoluchowski eq. $\Rightarrow z = d_f(1+\alpha) - (d - d_w)$

Regular clusters $M < \overline{M}$

$d_f = d = d_w = 2$

$\alpha = 0.5$

$z = 2(1+0.5) = 3$

Fractal clusters $M > \overline{M}$

$d_f = 1.45, d = 2$ and $d_w \sim 2$

if, instead, $\boxed{\alpha = 1}$

$z = 1.45(1+1) \sim 3$

Reviews on the application of fractals to colloidal aggregation

R. Jullien, Croatia Chemica Acta 65, 215 (1992) P. Meakin, Physica Scripta 46, 295 (1992)

Freezing/Melting - arrows

Hexatic (orientational) order parameter $\psi_{6j} = \frac{1}{nn_j}\sum_{k=1}^{nn_j} e^{i6\theta_{jk}}$

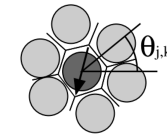

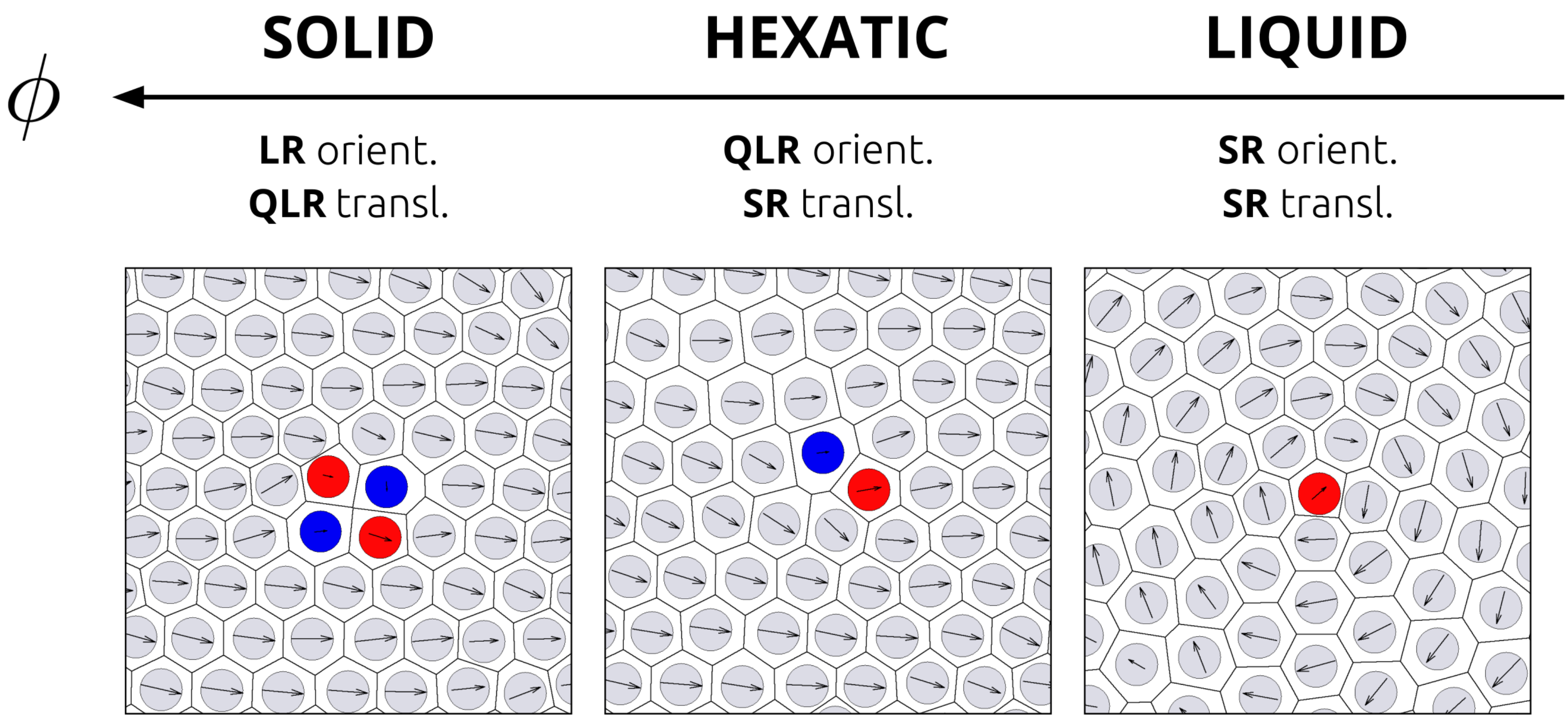

arrows oriented (LR) less oriented (QLR) order lost (SRL)

● five neighbours ● seven neighbours

Voronoi tessellation

Phases & transitions

$2d$ passive Pe = 0 systems: BKT-HNY *vs.* a new scenario

	BKT-HNY	BK
Solid	QLR pos & LR orient	QLR pos & LR orient
transition	BKT	BKT
Hexatic	SR pos & QLR orient	SR pos & QLR orient
transition	BKT	**1st order**
Liquid	SR pos & orient	SR pos & orient

Basically, the phases are the same, but the **hexatic**-**liquid** transition is different, allowing for **coexistence of the two phases** for **hard enough particles**

Event driven MC simulations. **Bernard & Krauth PRL 107, 155704 (2011)**

Results I on ABPs

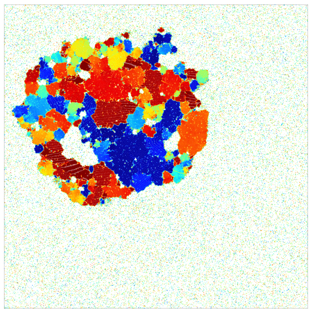

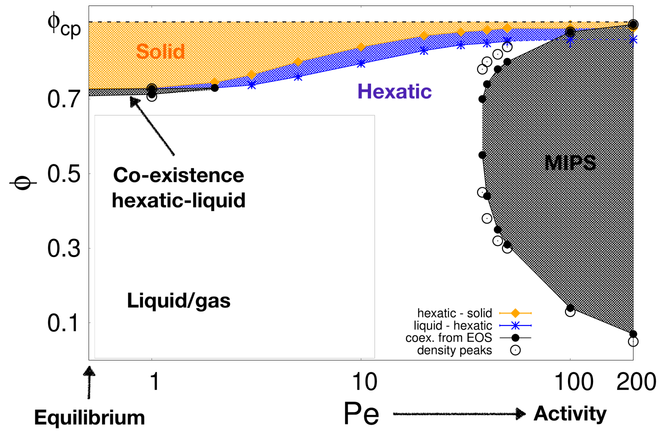

In **MIPS**

Ostwald ripening & Cluster-cluster aggregation

$R(t) \sim t^{1/3}$, $R_H(t) \sim t^{0.13}$

Micro *vs.* macro: hexatic patches & bubbles

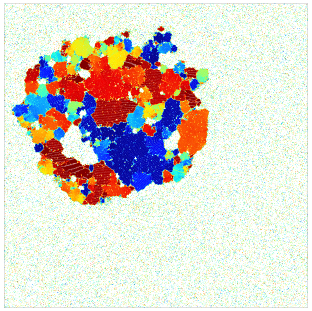

Results II on ABPs

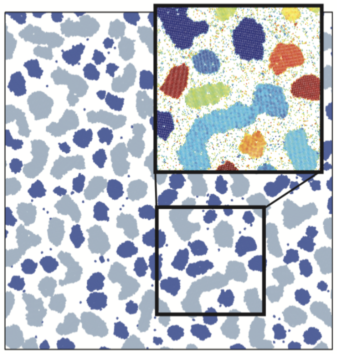

Difference between

Passive

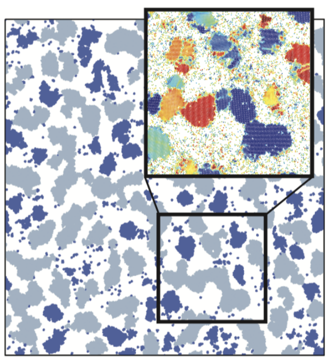

Active

growth

Ostwald ripening & cluster-cluster diffusive aggregation in active case
cluster-cluster aggregation almost not present in passive

Co-existence of regular and fractal clusters in both cases

Heterogeneous orientational order in large active clusters only